

Evaporative Cooling of Actuators for Humanoid Robots

Ulrich Hochberg, Armin Dietsche, Klaus Dorer

Hochschule Offenburg, Germany

Email: {Ulrich.Hochberg, Armin.Dietsche, Klaus.Dorer}@hs-offenburg.de

Abstract—Autonomous humanoid robots need high torque actuators to be able to walk and run. One problem in this context is the heat generated. In this paper we propose to use water evaporation to improve cooling of the motors. Simulations based on thermodynamic calculations as well as measurements on real actuators show that, under the assumption of the load of a soccer game, cooling can be considerably improved with relatively small amounts of water.

I. INTRODUCTION

Since 2002 humanoid robots participate in the RoboCup competition. Robots of increasing size and weight are to be found in the KidSize, TeenSize and AdultSize leagues [1]. For soccer playing especially, in the bigger size leagues, autonomous humanoid robots need high torque actuators to walk, run and kick. A conflicting requirement is the lightweight design of the actuators. Efficient cooling increases the maximum continuous torque of an electrical actuator, unfortunately most cooling systems increase the total weight of the robot dramatically. A heat pipe for motor cooling is described in [2]. A harmonic drive increases maximum torque but imposes a problem with internal cooling [3]. Introducing a circuit of cooling liquid helps to increase torque [4]. Liquid cooled motors in humanoid robotic application also increases the peak torque as well as the maximum output torque [5]. A bionic approach to an efficient lightweight cooling system is evaporative cooling: the actuators are cooled by evaporating water - similar to the cooling of muscles of a human being [6].

The remainder of this paper is organized as follows: In Section II we describe the theoretical thermodynamic background of evaporative cooling of actuators. Section III focuses on the setup and assumptions of the simulation as well as the real measurements. Section IV summarizes the experimental results before we conclude in Section V. The nomenclature used during this paper is shown in the Appendix.

II. THEORETICAL BACKGROUND

This section describes the heat dissipation in an actuator, the thermodynamic equations for the heat flux and the transient model of the motor used for later simulations.

A. Heat Dissipation of Brushed and Brushless DC-Motors

At least a part of the electrical energy transferred to the motor is dissipated and has to be removed by cooling. The main reasons for the heat production are the electrical resistance of the windings, eddy currents in the conductive parts of the stator and - in case of brushed DC-motors - resistance and sparks in the collector due to the inductivity of

the windings. In high loaded actuators the electrical resistance of the windings is dominant, in a first approach the other factors can be neglected. Another crude simplification is that the torque M of the motor is proportional to the current in the winding I , thus giving with Ohms's law the heat flux that is produced \dot{Q}

$$\dot{Q} \propto M^2 \quad (1)$$

This heat has to be removed from the motor, and in many typical applications the produced heat is the limiting factor for the average torque. [6]

It should be pointed out that in a first approximation this heat does not depend on the speed of the motor, it only depends on the torque. Even at zero speed (where the motor does not release any mechanical power) this heat is produced. In other words: if the actuator just has to hold the actual position of a joint, the mechanical efficiency of the motor is zero and all electrical energy which is needed to keep the position is transferred into heat. [5]

B. Thermodynamics of Conductive / Convective Cooling

The heat is produced in the windings and has to be transported to the environment. The relevant heat transfer coefficients are α_{wh} between the windings and the housing of the motor, α_{hc} between the housing of the motor and the case of the actuator and α_{ca} between the case of the actuator and the surrounding air. In case of the surfaces A between winding and housing, housing and body and to the environmental air are of the same size, the equation for the heat in steady state conditions is

$$\dot{Q}_c/A = \alpha_{wh}(\vartheta_w - \vartheta_h) = \alpha_{hc}(\vartheta_h - \vartheta_c) = \alpha_{ca}(\vartheta_c - \vartheta_a) \quad (2)$$

whereas $\vartheta_w, \vartheta_h, \vartheta_c, \vartheta_a$ are the temperature of the winding, the housing of the motor, the case of the actuator and the ambient air respectively.

Figure 1 schematically shows the structure of an actuator which is widely used for robots in the soccer competition.

For the sake of convenience the heat transfer coefficients are combined to one overall heat transfer coefficient U

$$U = \frac{1}{1/\alpha_{wh} + 1/\alpha_{hc} + 1/\alpha_{ca}} \quad (3)$$

Equation 2 can then be rearranged to calculate the temperature of the windings:

$$\vartheta_w = \vartheta_a + \dot{Q}_c/A/U \quad (4)$$

The temperature of the windings must not exceed a maximum temperature which is given by the design of the motor. Typically the heat transfer coefficients α_{hc} and α_{ca} are smaller than α_{wh} , dominating the denominator of equation 3. A significant increase of this heat transfer coefficient would enable a substantial higher heat flux \dot{Q} for the same temperature of the winding ϑ_w and thus allow a higher maximum continuous torque.

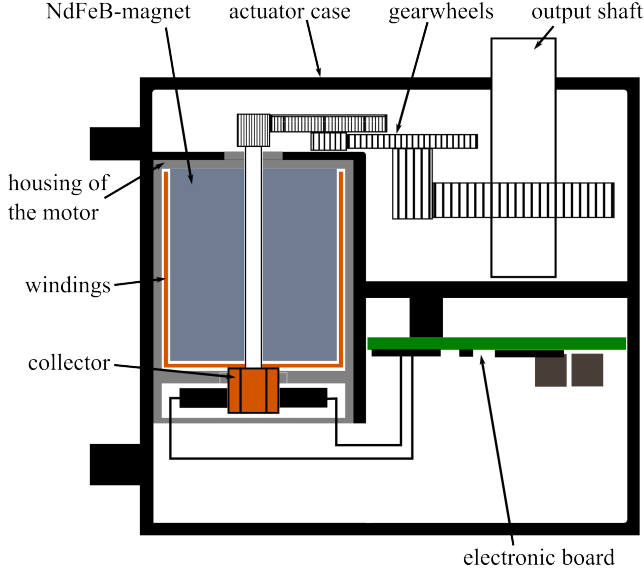


Fig. 1. Layout of simplified Dynamixel MX-106 Actuator.

C. Thermodynamics of Evaporative Cooling

While there has to be a temperature difference to transfer heat in conductive or convective cooling, there is no need for a temperature difference for evaporative heat transfer.

The dominating equation for the heat transfer by evaporative cooling is

$$\dot{Q}_e = \dot{M} \cdot \Delta h_v \quad (5)$$

where \dot{Q}_e denotes the heatflux due to evaporation, \dot{M} is the mass flow of the evaporated liquid and Δh_v is the specific heat of evaporation.

The mass flow of the evaporated liquid depends on the difference of the partial pressure of the water at the phase boundary p_{Ph} and the partial pressure of the water in the environment p_∞ [7].

Analogous to the heat transfer the mass transfer is calculated according to

$$\dot{M} = \rho \cdot \beta \cdot A \cdot (y_{Ph} - y_\infty) \quad (6)$$

whereas ρ is the density of the gas, β the mass transfer coefficient and y_{Ph} and y_∞ are the molar fractions of the water at the phase boundary and sufficiently far away respectively.

The molar fraction of water at the phase boundary y_{Ph} is calculated assuming thermodynamic equilibrium between fleece temperature ϑ_{fl} and p_{Ph} . The saturation pressure p_{Ph} is calculated using the Antoine-equation

$$y_{Ph} = \frac{p_{Ph}}{p} \quad (7)$$

whereas the coefficients a , b and c can be found in literature [8]. The molare fraction is the ration of the partial pressure of the water to the total pressure p .

$$\ln p_{Ph} = a - \frac{b}{c + \vartheta_{fl}} \quad (8)$$

The partial pressure of water in a distance sufficiently far away y_∞ is calculated from the room temperature ϑ_∞ and the relative humidity of the room ϕ_∞ , again using the Antoine equation.

The mass transfer coefficient β can be calculated from the Sherwood number Sh

$$\beta = \delta / l \cdot Sh \quad (9)$$

The diffusion coefficient for water in air δ can be found in literature, as well as the other properties [7]. The Sherwood number Sh depends, in case of free convection, on the Grashof number Gr and the Schmidt number Sc . The Schmidt number Sc for water in air is similar to the Prandtl number Pr (0.6 versus 0.7). Therefore the Sh number can be calculated in analogy to the Nu number according to the empirical equation [7]

$$Sh \approx Nu \approx [0.825 + 0.323Ra]^2 \quad (10)$$

The Rayleigh number describes the free convection introduced by the lower density of the gas at the phase boundary versus the density far away:

$$Ra = \frac{gl^3}{\nu^2} \cdot \frac{\rho_\infty - \rho_{Ph}}{\rho_\infty} \cdot Pr \quad (11)$$

Finally, at higher temperatures, the Stephan-correction has to be taken into account: similar to condensation [9] there is an overall massflow perpendicular to the mass transfer area A which increases the mass transfer by more than 20% at 70°C and can be calculated according to

$$\ln \frac{1 - y_\infty}{1 - y_{Ph}} \quad (12)$$

With this set of equations we calculated the evaporated mass flow $\dot{M} = f(\vartheta_{fl})$ in II-D

D. Transient Thermal Model

Based on the equations in II-B the convective heat flux \dot{Q}_c can be calculated as a function of the temperature of the case ϑ_c . The evaporative heat flux \dot{Q}_e can be calculated according to the equations given in II-C depending on the temperature of the cooling fin ϑ_{fl} . Figure 2 shows a transient thermal model of the MX-106 servomotor equipped with a cooling fin for evaporative heat transfer. The model is set up with Matlab/Simulink®. Input parameter is the heat dissipation in the windings of the motor (1). The temperature difference (4) causes a heat flow from the windings (3) to the housing of the motor (7). One part of the thermal flow heats up the cooling fin which can evaporate water. The other part of the thermal flow heats up the case of the actuator. The case conducts the heat only by convective heat transfer. The coefficient for describing the conductive heat transfer from the housing to the case (transfer function case1) is unknown and has to be

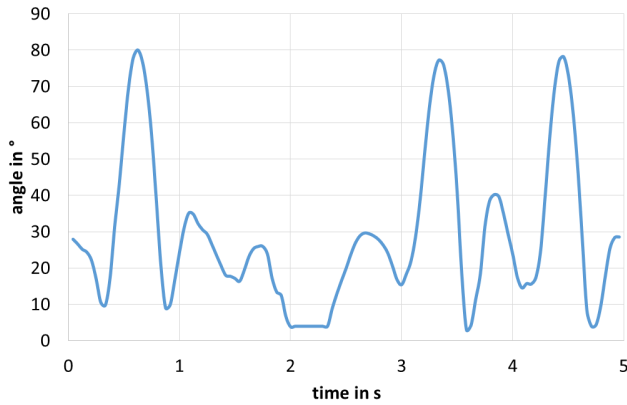


Fig. 3. Knee pitch over time from motion capturing file.

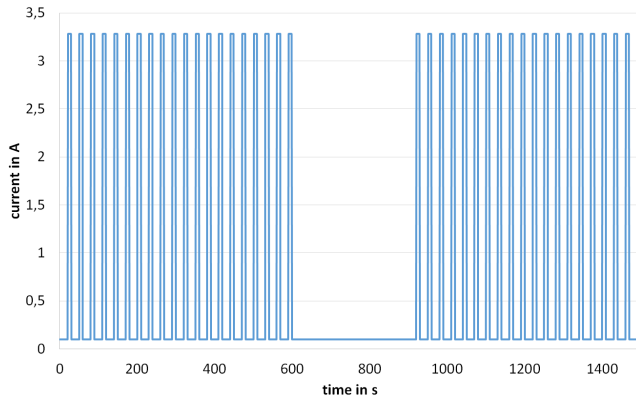


Fig. 4. Assumed current in knee actuator during a RoboCup game.

Maxon Motor RE-max 24 servomotors [13]. With a gear ratio of 225 and an assumed gear efficiency of 1 the estimated average momentum in the motor is 35 mNm while walking and 1 mNm while standing. The torque constant of the Maxon Motor RE-max 24 is 10.4 mNmA^{-1} . This causes a current of 3.4 A while walking and 0.1 A while standing still. With these currents the same heat is produced in the servomotor as it would be produced during the hypothetical game.

B. Hardware and Experimental Setup

A Robotis Dynamixel MX-106R actuator [12] has been modified for evaporative cooling purposes. To generate good thermal conduction from the housing of the motor to the environment the motor has been coated with three layers of aluminum foil-strips with a thickness of respectively 0.15 mm. Both ends of each aluminum-stripe are sticking out on the front side of the actuator case.

To make room for these head conduction structures the case of the actuator has been machined with a CNC milling machine. The diameter of the cylindrical bore hole, which is the seat of the motor case, has been partly increased to 25 mm. Furthermore a furrow has been created on the short side of the actuator case which is the through-passage region for the aluminum-strips. On the outside the case of the actuator these stripes are jacketed in water-damped fleece where the evaporation takes place. The fleece is a PET-fleece which is coated to be hydrophilic. It has very a high water adsorption

capacity while having low capillary forces.

For the test the motor has been supplied with electrical energy directly, i.e. without the help of the standard control board. During the experiment the output shaft of the actuator has been blocked. This means all of the supplied electrical energy dissipates into thermal energy. This blocking has been realized by a plate which has the same width as the gear housing of the actuator. This plate has been mounted to the output shaft via a horn. Thereafter the whole assembly has been clamped in a vice. To record the temperature a thermocouple has been fixed on the surface of the motor housing. The used thermocouple measurement chain (Ni-CrNi) has an overall accuracy of $\pm 1.5 \text{ K}$.

The motor has been supplied with electrical current according to the load profile determined above. The current has been measured with an accuracy of $\pm 0.01 \text{ A}$. The temperature of the motor housing has been recorded every 30 s. Figure 5 and 6 show the Dynamixel MX-106 actuator equipped with a straight cooling fin like it is used in our experiments.

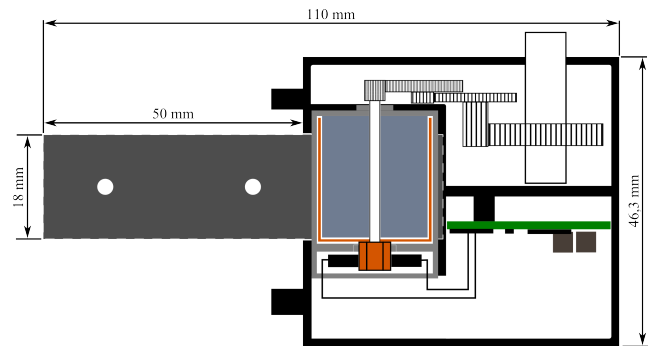


Fig. 5. Layout of simplified MX-106 with cooling fin.



Fig. 6. Modified actuator with cooling fin.

Because the transferred heat practically is only depending on the surface area of the cooling fin, the profile can adapted to save the constructed space, e.g. circular like in Figure 7.

IV. RESULTS

This section discusses the results of simulations of motor temperatures as well as measurements on real actuators with and without cooling.

A. Motor Temperature (Simulation)

The following coefficients required for the simulations have been ascertained in experiments: Heat capacities:

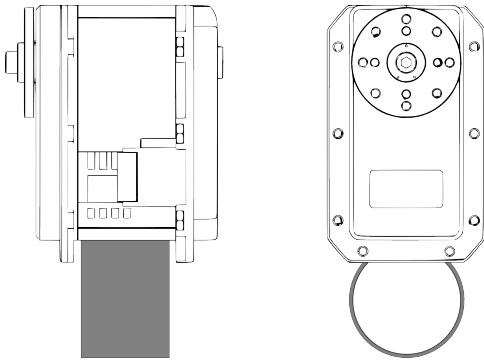


Fig. 7. Circular cooling fin to save constructed space.

- Windings: 1.631 J K^{-1}
- Housing (Maxon): 53.63 J K^{-1}
- Case (Dynamixel): 96.15 J K^{-1}
- Cooling fin: 3.32 J K^{-1}

Thermal conductance:

- Windings to housing: 0.1961 WK^{-1}
- Housing to case: 0.07 WK^{-1}
- Housing to cooling fin: 0.17 WK^{-1}

The temperature at the start is set to 25°C (Initial condition for Integrator function).

Figure 8 shows the temperature profile of the unmodified actuator and compares the results of the experiment and the simulation. The data has been used to determine the heat capacity of the housing of the motor and the thermal conductance between housing and case. With a maximum deviation of about 2°C the compliance between the experimental results and the simulation is very high. The blue line in Figure 9 shows the enhanced simulation with evaporative cooling based on the coefficients determined in the experiment before. The deviation between the calculated temperature and the experimental data is negligible.

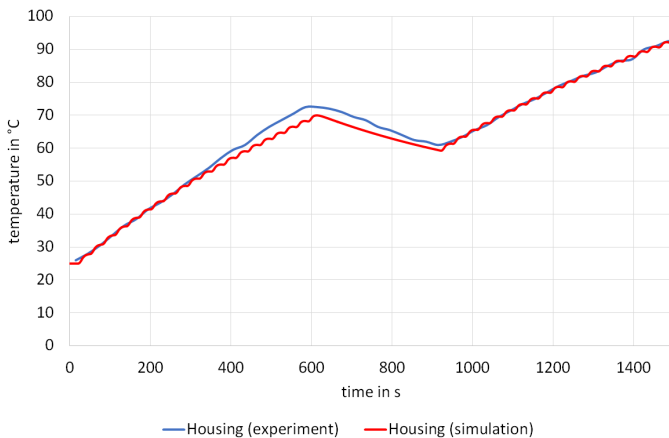


Fig. 8. Comparison of simulation and measurement of housing temperature.

B. Motor Temperature (Experiment)

The transient momentum according to Section III has been applied to an unmodified and a modified MX-106 actuator (Figure 6) with and without cooling. Robotis defines an upper limit for the housing temperature of 80°C [12].

Figure 8 shows the results of the experiment with the unmodified actuator (red line). In the first halftime the housing temperature is rising to almost 75°C . After cooling down to about 60°C during the 5 minutes break, the temperature reaches the 80°C limit in the middle of the second half and is not able to play for the last 5 minutes of the game.

The orange line shows the temperature profile during the game when the motor is equipped with the cooling fin. The heat transfer to the air is only by convective cooling. The results show that the temperatures of the housing are a bit lower, especially at the end of the game. Nevertheless, the 80°C limit is exceeded about two minutes before finishing the second halftime.

If the cooling fin is equipped with the wet fleece, the heat transfer can be realized by evaporative cooling (blue and green line). Because of the higher heat transfer to the air due to the evaporation of water compared with the convective cooling, the maximum temperature in the first halftime is only about 55°C and at the end of the second halftime at about 63°C . This means the robot is able to play the whole game and there are still power reserves when using the above load profile.

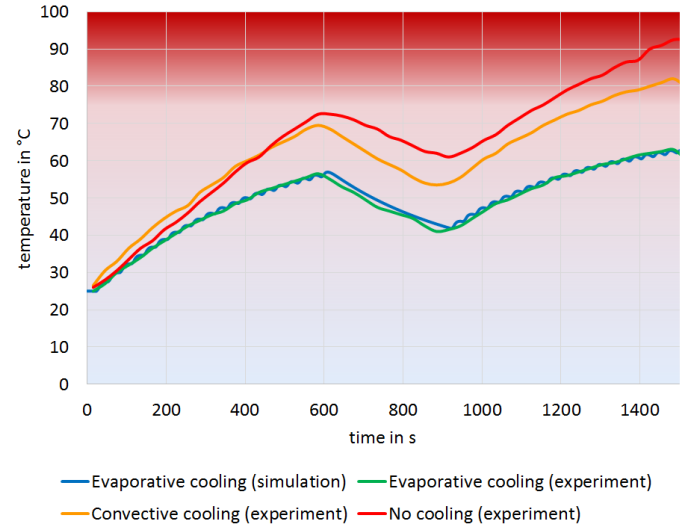


Fig. 9. Temperature of the housing of the motor with and without cooling.

C. Evaporated Water

1) *Analytical:* The defined hypothetical game consists of 40 load-cycles of 9 s with a current of 3.28 A. The used Maxon Motor RE-max 24 has an inner resistance of 1.78Ω . This results in a power dissipation of 18.6 W while the actuator is loaded. With an efficiency of the actuator of 0%, i.e. all electric energy is dissipated as a consequence, this leads to a produced heat of 6700 J. Water has a specific heat of evaporation of 2400 kJ kg^{-1} . In this worst case scenario, the dissipated electric energy can evaporate a mass of water of $6.7 \text{ kJ} / 2400 \text{ kJ kg}^{-1} = 2.8 \text{ g}$. With the specified load profile

for the hypothetical game the system is not in steady state conditions at the end of the game. Thus, a large amount of the energy heats up the housing, the case and the cooling fin and is not evaporating water.

2) *Numerical*: During the simulation the evaporative heat flow is calculated (signal 12 in Fig. 2). By integrating the heat flow, the amount of energy transferred by evaporative cooling can be calculated according to

$$Q_e = \int \dot{Q}_e dt \quad (13)$$

The result of the simulation is $Q_e = 2.71$ kJ. This leads to an evaporated mass of water of 1.13 g during the hypothetical game.

3) *Experiment*: The weight of the actuator was determined with an electronic balance having an accuracy of +/- 0.1g. The difference in weight before and after the experiment was 1.23 g. This is in good agreement with the calculated value. As the fleece can adsorb 1.34 g of water there was no need to re-humidify it during the experiment.

V. CONCLUSION AND FUTURE WORK

In this paper we have shown that water evaporation can be efficiently used to reduce the temperature of servo motors during the load of a RoboCup game with less than 2 grams of water. There is no need to re-humidify the actuator during a game. Motor temperatures can theoretically be predicted in good agreement with the actual figures. Possible alternatives to evaporative cooling could be active cooling by a fan, using a small metal block as a heat sink or just using a stronger actuator. In all three cases the weight would increase considerably. Furthermore these alternative cooling systems would need a bigger constructed space. The weight of an actuator modified for evaporative cooling is only 2% higher than the weight of an unmodified actuator. Thus the evaporative cooling system can enhance the power of endurance of Kid-Size, Teen-Size and Adult-Size robots almost without increasing weight.

A limiting factor for the load of a motor is the temperature of the windings. This temperature will be the focus of further research. The temperature of the windings can be predicted very precisely. Therefore the decisions of the movements for the robots can be made not only based on the actual game situation but also based on the thermal status of the robot - just like a real soccer player bases his decisions on his actual physical shape.

ACKNOWLEDGMENT

The authors would like to thank the Hochschule Offenburg for the financial support of the project.

REFERENCES

- [1] S. Behnke, M. Schreiber, J. Stuckler, R. Renner, and H. Strasdat, "See, walk, and kick: Humanoid robots start to play soccer," in *Humanoid Robots, 2006 6th IEEE-RAS International Conference on*, 2006, pp. 497–503.
- [2] G. Binder and G. Woessner, "Kuehlvorrichtung fuer elektrische maschinen," DE Application 2 810 222, 1979.
- [3] R. Crowder, "The application and control of brushless dc motors in high power robotic joints," in *Power Electronics and Variable-Speed Drives, Third International Conference on*, 1988, pp. 253–256.

- [4] K. Hwang, S. W. Lee, S. W. Karng, and S. Y. Kim, "Thermal performance of non-metallic two-phase cold plates for humanoid robot cooling," in *Thermal and Thermomechanical Phenomena in Electronic Systems, 2008. ITherm 2008. 11th Intersociety Conference on*, 2008, pp. 6–11.
- [5] J. Urata, Y. Nakanishi, K. Okada, and M. Inaba, "Design of high torque and high speed leg module for high power humanoid," in *Intelligent Robots and Systems (IROS), 2010 IEEE/RSJ International Conference on*, 2010, pp. 4497–4502.
- [6] U. Hochberg and N. Jahn, "Electromotive actuator of mobile robot e.g. humanoid robot," DE Patent Application 102 011 054 727A1, 2013.
- [7] *VDI-Waermeatlas: Berechnungsblaetter fuer den Waermeuebergang*, 9th ed. Berlin ; Heidelberg [u.a.]: Springer Dordrecht, 2002.
- [8] J. Gmehling, U. Onken, W. Arlt, P. Grenzheuser, U. Weidlich, U. Kolbe, and J. Rarey, *Chemistry Data Series, Volume I*. Dechema, 1991 - 2010.
- [9] U. Hochberg, "J4 mixing and spray condensation," in *VDI Heat Atlas*, ser. VDI-Buch. Springer Berlin Heidelberg, 2010, pp. 939–944.
- [10] "Robocup soccer humanoid league rules and setup 2013," <http://www.tzi.de/humanoid/pub/Website/Downloads/>, last visited: 2013-09-14.
- [11] B. MOTION, "Walk turn 180," <http://www.beyondmotion.com.au/>, last visited: 2013-09-14.
- [12] "Robotis e-manual," <http://support.robotis.com/en/>, last visited: 2013-09-14.
- [13] Maxon, "Motor spec.re-max 24," <http://www.maxonmotor.de/>, last visited: 2013-09-14.

APPENDIX

TABLE I. SYMBOLS USED IN FORMULAS.

Symbol	Unit	Semantics
A	m^2	heat and mass transfer area
M	Nm	torque of the motor
\dot{M}	kgs^{-1}	mass flow of evaporated liquid
\dot{Q}	W	total heat flux
\dot{Q}_c	W	conductive and convective heat flux
\dot{Q}_e	W	heat flux due to evaporation
Q_e	J	total heat transferred by evaporative cooling
U	$Wm^{-2}K^{-1}$	overall heat transfer coefficient
a, b, c		constants of the Antoine equation
g	$m s^{-2}$	gravity constant
l	m	characteristic (vertical) length of the cooling fin
p	Pa	total pressure
p_{Ph}	Pa	partial water pressure at phase boundary
p_∞	Pa	partial water pressure in a sufficiently far distance
y_{Ph}	-	molar fraction of water at phase boundary
y_∞	-	molar fraction of water in a sufficiently far distance
α_{wh}	$Wm^{-2}K^{-1}$	heat transfer coefficient (htc) winding/housing of the motor
α_{hc}	$Wm^{-2}K^{-1}$	htc housing of the motor / case of the actuator
α_{ca}	$Wm^{-2}K^{-1}$	htc case of the actuator / air
β	ms^{-1}	mass transfer coefficient
Δh_v	Jkg^{-1}	specific heat of evaporation
δ	m^2s^{-1}	diffusion coefficient of water in air
ϑ_∞	-	relative humidity in a sufficiently far distance
ϑ_h	K	temperature of the housing of the motor
ϑ_w	K	temperature of the winding
ϑ_c	K	temperature of the case of the actuator
ϑ_{fl}	K	temperature of the case of the cooling fluid / cooling fin
ϑ_a	K	temperature of the air (ambient temperature)
ρ	$kg m^{-3}$	gas density
ν	m^2s^{-1}	kinematic viscosity of the air
Nu	-	Nusselt number
Pr	-	Prandlt number
Ra	-	Raleigh number
Sh	-	Sherwood number